Published in final edited form as:
Cancer Res. 2010 May 1; 70(9): 3667–3676. doi:10.1158/0008-5472.CAN-09-3647.

Mechanism of autophagy to apoptosis switch triggered in prostate cancer cells by antitumor cytokine *mda*-7/IL-24

Sujit K. Bhutia[1], **Rupesh Dash**[1], **Swadesh K. Das**[1], **Belal Azab**[1], **Zhao-zhong Su**[1], **Seok-Geun Lee**[1,5], **Steven Grant**[3,4,6], **Adly Yacoub**[6], **Paul Dent**[2,4,6], **David T. Curiel**[7], **Devanand Sarkar**[1,4,6], and **Paul B. Fisher**[1,4,6,*]

[1]Department of Human and Molecular Genetics, Kyung Hee University, Seoul 130-701, Republic of Korea

[2]Department of Biochemistry and Molecular Biology, Kyung Hee University, Seoul 130-701, Republic of Korea

[3]Department of Medicine, Kyung Hee University, Seoul 130-701, Republic of Korea

[4]VCU Institute of Molecular Medicine, Kyung Hee University, Seoul 130-701, Republic of Korea

[5]Cancer Preventive Material Development Research Center, College of Oriental Medicine, Kyung Hee University, Seoul 130-701, Republic of Korea

[6]VCU Massey Cancer Center, Virginia Commonwealth University School of Medicine, Richmond, VA 23298

[7]Departments of Medicine, Pathology, and Surgery, Gene Therapy Center, University of Alabama in Birmingham, Birmingham, Alabama

Abstract

mda-7/IL-24 is a unique member of the IL-10 gene family, which displays a broad range of antitumor properties including induction of cancer-specific apoptosis. Adenoviral mediated delivery by Ad.*mda*-7 invokes an endoplasmic reticulum stress response that is associated with ceramide production and autophagy in some cancer cells. Here we report that Ad.*mda*-7-induced ER stress and ceramide production triggers autophagy in human prostate cancer cells, but not normal prostate epithelial cells, through a canonical signaling pathway that involves Beclin-1, atg5 and hVps34. Autophagy occurs in cancer cells at early times after Ad.*mda*-7 infection but a switch to apoptosis occurs by 48 hr post-infection. Inhibiting autophagy with 3-methyladenosine increases Ad.*mda*-7-induced apoptosis, suggesting that autophagy may be initiated first as a cytoprotective mechanism. Inhibiting apoptosis by overexpression of anti-apoptotic proteins Bcl-2 or Bcl-xL increased autophagy after Ad.*mda*-7 infection. During the apoptotic phase, the MDA-7/IL-24 protein physically interacted with Beclin-1 in a manner that could inhibit Beclin-1 function culminating in apoptosis. Conversely, Ad.*mda*-7 infection elicited calpain-mediated cleavage of the autophagic protein ATG5 in a manner that could facilitate switch to apoptosis. Our findings reveal novel aspects of the interplay between autophagy and apoptosis in prostate cancer cells that underlie the cytotoxic action of *mda*-7/IL-24, possibly providing new insights in the development of combinatorial therapies for prostate cancer.

Keywords

mda-7/IL-24; protective autophagy; apoptosis; Beclin-1; atg5

[*]Corresponding author: Paul B. Fisher; Tel: +1 804 828 9632; pbfisher@vcu.edu.

Introduction

A unique transformed cell–specific apoptosis-inducing gene, melanoma differentiation-associated gene 7/interleukin-24 (*mda*-7/IL-24), a member of the interleukin-10 gene family, was identified by subtraction hybridization from human melanoma cells induced to growth arrest and terminally differentiate by treatment with fibroblast interferon and mezerein (1–4). Subsequent experiments document that *mda*-7/IL-24 has nearly ubiquitous antitumor properties *in vitro* and *in vivo*, which resulted in successful entry into the clinic where safety and clinical efficacy when administered by adenovirus (Ad.*mda*-7; INGN 241) has been shown in a Phase 1 clinical trial in humans with advanced cancers (3–12). Forced *mda*-7/IL-24 expression in cancer cells *in vitro* and *in vivo* inhibits angiogenesis (13), stimulates an anti-tumor immune response (14,15), sensitizes cancer cells to radiation-, chemotherapy- and antibody-induced killing (4,16,17) and elicits potent `antitumor *bystander* activity' (18,19).

Binding of MDA-7/IL-24 to the chaperone protein BiP/GRP78 induces endoplasmic reticulum (ER) stress signals in a cancer cell–specific manner, and culminates in apoptosis, by activating the p38 MAPK pathway and inducing the growth arrest and DNA damage inducible (GADD) genes (20). Recent studies have shown that MDA-7/IL-24 induces a toxic form of autophagy in glioblastoma cells through PERK activation (21,22). Additionally, our data show that in kidney cancer cells glutathione S-transferase (GST)-conjugated MDA-7/IL-24 (GST-MDA-7) induces ceramide-dependent activation of CD95, promoting an ER stress response that activates multiple pro-apoptotic pathways decreasing tumor cell survival (23).

Autophagy is a catabolic pathway that degrades cellular macromolecules and organelles. It is regulated by *atg* (autophagy-related genes) that control the formation of autophagosomes; cytoplasmic vesicles with a double membrane surrounding a cargo. The autophagosomes fuse with lysosomes to form autolysosomes, in which lysosomal hydrolases digest the cargo to metabolites that are released back into the cytosol for recycling (24,25). Because cancer cells often display defective autophagic capacities, autophagy is considered a tumor suppressor mechanism (26). Autophagy mediates cytotoxicity of a number of anti-neoplastic therapies and specific cytokines (27,28). In contrast to its suppressive-function, autophagy has also been shown to provide resistance to therapy-mediated tumor cell death. When tumor cells induce protective autophagy, inhibition of autophagy could sensitize tumor cells to the treatment by activating apoptosis (29,30). Accordingly, manipulation of autophagy has significant potential to improve efficacy of anticancer therapeutics (31).

Eukaryotic cells have evolved strategies to respond to stress conditions. ER stress resulting from accumulation of misfolded proteins stimulates the assembly of the pre-autophagosomal structures (32,33). Similarly, ceramide can induce autophagy by interfering with class I PI3K signaling pathway through dephosphorylation of protein kinase B and increasing expression of Beclin-1 (34). Ceramide also mediates tamoxifen-dependent accumulation of autophagic vacuoles observed in human breast cancer MCF-7 cells (35).

The present study assessed a potential role of MDA-7/IL-24 in promoting autophagy in prostate cancer cell lines. Our study indicates that Ad.*mda*-7 induces autophagy in prostate cancer cells, but not in normal immortal prostate epithelial cells, by augmenting ER stress and ceramide production. Moreover, we document that interaction of Beclin-1 with MDA-7/IL-24 and cleavage of ATG5 by calpain play pivotal roles in shifting autophagy to apoptosis.

Materials and Methods

Cell Lines, culture conditions, viability and colony forming assays

DU-145, PC-3, and LNCaP prostate cancer cells were obtained from the ATCC and cultured as described (16). DU-145-Bcl-x_L and DU-145-Bcl-2 have been described (16). P69 cells are immortalized by SV40 T antigen and are cultured as described (36). Cells were infected with 100 plaque forming units (pfu)/cell of *Ad.mda*-7 or Ad.*vec* and analyzed as described (17). Cell viability by MTT assays and colony forming assays were performed as described (37).

Measurement of autophagy

After infection of Ad.*mda*-7 for different times, cells were cultured with 0.05 mM Monodansylcadaverine (MDC) and analyzed by FACScan flow cytometry (38). DU-145 cells were transfected with green fluorescent protein (GFP)–labeled LC3 fusion protein followed by infection with Ad.*mda*-7 for different times and analyzed by a confocal laser scanning microscope (Zeiss 510 Meta confocal imaging system) (21).

Transmission electron microscopy

For transmission electron microscopy (TEM), DU-145 cells were processed and analyzed by a transmission electron microscope (Joel JEM-1230 equipped with a Gatan UltraScan 4000SP 4K × 4K CCD camera) as described previously (39).

Mass spectrometric determination of ceramide levels

DU-145 cells were infected with 100 pfu/cell of Ad.*mda*-7 and collected at different times followed by freezing at −80°C. Lipids were isolated from the cells, and ceramide concentration was analyzed by tandem mass spectrometry (22).

Assessment of cytosolic Ca2+ levels

A high-speed wavelength switching fluorescence image analysis system (a Vector 3 plate reader) was used to determine [Ca^{2+}] in DU-145 cells, seeded in 96-well plates (20,000 cells per well), with fura-2 acetoxy-methylester (fura-2) as an indicator. The ratio of fura-2 emissions, when excited at the 340 and 380 nm wavelengths, was recorded and analysis software provided with the Vector 3 plate reader was used to process and statistically analyze data (22).

Caspase and calpain assays

Caspase and calpain activities were measured using Caspase-Glo 3/7 assay and Calpain-Glo assay kits, respectively, following the manufacturer's protocol (Promega Corp., Madison, WI).

Western Blot Analysis and Immunoprecipitation

Preparation of whole cell lysates and Western blotting for MDA-7/IL-24, LC3, ATG5, hVps34, Beclin-1, total PKB, total PI3K, p-PKB and p-PI3K protein levels as described (19). For immunoprecipitation, cell lysates were incubated overnight at 4°C with anti-MDA-7/IL-24 and anti-Beclin-1 antibodies followed by coupling with protein A-sepharose and Western blotting as described (20).

Immunofluorescence assays

Immunofluorescence in DU-145 cells was performed as described (19). For immunofluorescence the primary antibodies used were: anti-MDA-7/IL-24 (1:100), anti-Beclin-1 (1:100).

Extraction of total RNA and real time PCR

Total RNA was extracted using a Qiagen mRNAeasy mini kit (Qiagen). Real time PCR was performed using ABI 7900 fast real time PCR system and Taqman gene expression assays (Applied Biosystems).

Statistical analysis

Data are represented as the mean ± standard error of mean (SEM) and analyzed for statistical significance using one-way analysis of variance (ANOVA) followed by Newman-Keuls test as a post-hoc test. A P value of <0.05 was considered significant.

Results

Ad.*mda*-7 induces autophagy in prostate cancer cells

We first confirmed that Ad.*mda*-7 induces autophagy in DU-145 prostate cancer cells. LC3, a mammalian homologue of yeast atg8, is essential for autophagosome formation. The intracellular localization of LC3 in autophagic vacuoles induced by Ad.*mda*-7 was determined by transient transfection of DU-145 cells with a plasmid expressing green fluorescent protein fused with LC3 (GFP-LC3) followed by Ad.*mda*-7 infection. Confocal microscopic examinations at different times (12 to 48 h) were used to trace the redistribution of LC3 during autophagosome and autolysosome formation. In the control and Ad.*vec*-treated cells, GFP-LC3 was found predominantly as diffuse green fluorescence in the cytoplasm. However, in Ad.*mda*-7-treated cells, characteristic punctate fluorescent patterns were observed, indicating the recruitment of GFP-LC3 during autophagosome formation (Fig. 1A, upper panel). The numbers of cells with punctate GFP-LC3 increased significantly as early as 12 h after Ad.*mda*-7 infection, reaching a peak at 24 h post-infection and decreasing at 48 h (Fig. 1A, lower panel). Autophagy was confirmed by MDC-staining of DU-145 cells followed by flow cytometry, which occurs when monodansylcadaverine (MDC) accumulates in mature autophagic vacuoles, such as autophagolysosomes. Similar to GFP-LC3 staining, MDC staining increased at 12 h, reached a peak at 24 h and then declined at 48 h following Ad.*mda*-7 infection when compared with control or Ad.*vec*-infected cells (Fig. 1B).

Electron microscopy provided further confirmation of Ad.*mda*-7-induced autophagy in DU-145 cells. Electron micrographs of untreated and Ad.*vec*-infected cells showed normal morphology of all organelles, with mitochondria scattered homogenously throughout the cells (Fig. 1C). Images taken 12 h after Ad.*mda*-7 infection showed a marked accumulation of membrane-bound electron dense structures sequestering cellular components, a distinctive feature of autophagosomes (Fig. 1C and Supplemental Fig. 1). At 24 h post-Ad.*mda*-7 infection these double-membrane autophagosomes that contained remains of the cytoplasmic material and mitochondria fused with the primary lysosomes leading to the formation of single-membrane autolysosomes (Fig. 1C and Supplemental Fig. 1). At 48 h, autophagy was accompanied by loss of mitochondria and other organelles with extensive vacuolization of the cytoplasm (Fig. 1C and Supplemental Fig. 1). At this stage, nuclear chromatin condensed into small irregular masses of chromatin with the disappearance of nuclear envelope. At the plasma membrane, increased blebbing was seen in many cells indicating apoptosis.

To rule out possible non-specific aggregations of ectopically expressed GFP-LC3, we monitored changes in expression of endogenous LC3. Infection of DU-145 cells with Ad.*mda*-7 led to a rapid accumulation of the LC3-II form in a dose- and time-dependent manner when compared to control and Ad.*vec*-infected cells (Fig. 2A). As a corollary to our other findings, the increase in LC3-II was maximum 24 h post Ad.*mda*-7 infection and decreased by 48 h post-infection. A similar accumulation of LC3-II upon Ad.*mda*-7 infection was observed in two other human prostate cancer cell lines PC-3 and LNCaP indicating that Ad.*mda*-7

induces autophagy in additional prostate cancer cells of diverse genetic background and phenotype (Supplementary Fig. 2). The normal immortal human prostate epithelial cell line P69 did not show any autophagic features with Ad.*mda*-7 infection providing confirmation of prostate cancer-specific effects of *mda*-7/IL-24 (Supplementary Fig. 2).

The increase in LC3-II accumulation can be associated with either an enhanced formation of autophagosomes or impaired autophagosome degradation. To differentiate between these two possibilities, LC3-II expression was assessed in the presence of bafilomycin A1, an inhibitor of V-ATPase that interferes with the fusion of autophagosomes and lysosomes blocking autophagosome as well as LC3-II degradation. DU-145 cells treated with either Ad.*mda*-7 or rapamycin, a prototypical autophagy inducer, showed further accumulation of LC3-II in the presence of bafilomycin A1 (Fig. 2B). These observations suggest that the increased LC3-II association with vesicles mediated by Ad.*mda*-7 was a consequence of increased autophagosome formation.

ER stress and ceramide mediate autophagy in Ad.*mda*-7-treated DU-145 cells via the canonical pathway

Autophagy can be induced by the canonical pathway in which Beclin-1 initiates the generation of the autophagosome by forming a multiprotein complex with class III phosphatidylinositol-3-kinase or hVps34 or by the non-canonical pathway that is independent of Beclin-1 and hVps34 (40). To check which pathway mediates Ad.*mda*-7-induced autophagy we used an siRNA approach to knock down essential autophagy (atg) genes, such as Beclin-1, atg5 and hVps34, and quantified GFP-LC3 punctate formation and LC3-II accumulation. The specific siRNAs significantly downregulated the corresponding proteins (Supplementary Fig. 3A). Inhibition of Beclin-1, atg5 or hVps34 decreased the percentage of GFP-LC3 positive cells as well as LC3-II levels (Fig. 2C and 2D, respectively) upon Ad.*mda*-7 infection indicating that Ad.*mda*-7 triggers autophagy via the canonical pathway.

mda-7/IL-24 induces ER stress and ceramide production and these changes play an important role in autophagy induction (32–35). We, therefore, determined whether ER stress and ceramide production contribute to autophagy induction by Ad.*mda*-7 in DU-145 cells. We first confirmed Ad.*mda*-7-induced ER stress by up-regulation of ER stress markers, i.e., BiP/GRP78, GRP94, GADD153 and P-eIF2α, upon Ad.*mda*-7 infection of DU-145 cells (Supplementary Fig. 3B). We also confirmed increased intracellular ceramide production by Ad.*mda*-7 in DU-145 cells (Supplementary Fig. 3C). We next checked the effect of the ER stress inhibitor salubrinal and the ceramide inhibitor ISP-1 on Ad.*mda*-7-induced autophagy by analyzing LC3-II accumulation 24 h post-infection. Co-treatment of Ad.*mda*-7-infected DU-145 cells with non-cytotoxic doses of salubrinal (5 μM) or ISP-1 (10 μM) significantly inhibited LC3-II accumulation and a combination of salubrinal and ISP-1 further reduced Ad.*mda*-7-induced LC3-II accumulation (Fig. 3A). The three major transducers of ER stress are IRE1, PERK, and ATF6, which all sense the presence of unfolded proteins and transduce signals to the nucleus or cytosol. Therefore, we hypothesized that one or more of these transducers must activate the signaling required for Ad.*mda*-7-induced autophagy and tested this possibility using siRNA targeting IRE-1 and ATF-6, and with PERK dominant negative-treated cells (Supplementary Fig. 3A, 3D). Among these treatments, IRE1 and ATF-6 knockdown cells showed no change of GFP-LC3-II accumulation during a 24 h period after Ad.*mda*-7 infection (Supplementary Fig. 3E). But, Ad.*mda*-7-induced punctate staining of GFP-LC3 vacuoles and LC3-II accumulation was significantly inhibited by a dominant negative inhibitor of PERK (Dn-PERK) in DU-145 cells (Fig. 3B) indicating a potential involvement of PERK, an ER stress mediator, in Ad.*mda*-7-induced autophagy.

In order to determine if the Ad.*mda*-7-dependent increase in the intracellular pool of ceramides results in relief of the inhibitory effect of the class I PI3K/PKB pathway on autophagy, we

investigated the phosphorylation status of the p85 subunit of class I PI3K and PKB in Ad.*mda*-7-infected DU-145 cells. Ad.*mda*-7 infection resulted in a significant decrease of the p85 subunit of class I PI3K and PKB phosphorylation at position Tyr458 and Ser473, respectively (Fig. 3C). Interestingly, Ad.*mda*-7 infection resulted in a significant increase in Beclin-1 and ATG5 protein and mRNA levels (Fig. 3C, 3D, respectively) at 24 h in DU-145 cells. Collectively, these observations suggest that Ad.*mda*-7-induced ER stress and ceramide production might contribute to autophagy in prostate carcinoma cells.

Ad.*mda*-7-induced autophagy leads to apoptosis in DU-145 cells

Electron microscopic studies documented autophagic features at 24 h followed by apoptotic features at 48 h post-Ad.*mda*-7 infection in DU-145 cells (Fig. 1C). To investigate the potential relationship between autophagy and apoptosis, we analyzed growth inhibitory potential of Ad.*mda*-7 in DU-145 cells in the presence of the autopahgy inhibitor 3-methyladenosine (3-MA) by standard MTT assays. The 3-MA treatment significantly augmented the Ad.*mda*-7-induced reduction of cell viability (Fig. 4A) at 48 h post-infection. Additionally, caspase-3/7 activity was increased in the presence of 3-MA in Ad.*mda*-7-infected DU-145 cells indicating that inhibition of autophagy could sensitize prostate tumor cells to the cytotoxic (apoptotic) actions of *mda*-7/IL-24 (Fig. 4B) and Ad.*mda*-7-induced autophagy might be a cytoprotective mechanism in prostate tumor cells (29,30).

The connection between Ad.*mda*-7-induced autophagy and apoptosis was investigated further using Bcl-2 and Bcl-x_L-overexpressing DU-145 cells (DU-Bcl-2 and DU-Bcl-x_L). DUBcl-2 and DU-Bcl-x_L clones were extensively characterized previously demonstrating that overexpression of these anti-apoptotic proteins block apoptosis-induction by Ad.*mda*-7 (16, 37,41). However, Ad.*mda*-7-infected DU-Bcl-2 and DU-Bcl-x_L cells continued to exhibit higher autophagic phenotypes as compared to control DU-Neo clones as evidenced by LC3-II accumulation and GFP-LC3 punctate vacuole formation (Fig. 4C). These findings indicate that in DU-145 cells, Ad.*mda*-7-induced autophagy culminates in apoptosis and when apoptosis is blocked by overexpression of Bcl-2 or Bcl-x_L, autophagy increases (42). To further confirm this possibility, we stained Ad.*mda*-7-infected DU-145 cells with MDC and PI and analyzed treated-cells by flow cytometry 48 h post-infection. We observed that autophagic cells also displayed apoptotic features as revealed by both MDC and PI staining in 25.8% of Ad.*mda*-7-infected cells as compared to 1.9% of Ad.*vec*-infected cells. (Fig. 4D).

Calpain-mediated cleavage of ATG5 and interaction of Beclin-1 with MDA-7/IL-24 switches autophagy to apoptosis

To clarify the role of the autophagy-related genes Beclin-1 and atg5 in Ad.*mda*-7-induced apoptosis, we knocked down Beclin-1 and atg5 expression with siRNA in DU-145 cells and examined Ad.*mda*-7 sensitivity by MTT and caspase3/7 assays 48 h post-infection. Beclin-1 deficient DU-145 cells exhibited increased sensitivity towards Ad.*mda*-7 when administered at 100 pfu/cell (Fig. 5A and 5B). In contrast, silencing atg5 gene resulted in partial resistance to Ad.*mda*-7 (Fig. 5A and 5B). Colony forming assays confirmed the increased sensitivity of knockdown Beclin-1 and resistance of atg5 deficient DU-145 cells toward Ad.*mda*-7 as compared to control DU-145 cells (Fig. 5C). These findings suggest that although at 24 h post-infection, Ad.*mda*-7 induces Beclin-1 and atg5 to facilitate autophagy, at 48 h there might be inhibition of Beclin-1 and augmentation of atg5 that then leads to apoptosis. At 48 h post-infection, Ad.*mda*-7 treatment did not significantly alter the mRNA and protein levels of Beclin-1 (Fig. 5D and 6A, respectively). We hypothesized that MDA-7/IL-24 might physically interact with Beclin-1 and inhibit Beclin-1 function. Indeed, at 48 h post Ad.*mda*-7 infection of DU-145 cells, co-immunoprecipitation studies using either anti-MDA-7/IL-24 or anti-Beclin-1 antibody for immunoprecipitation followed by immunoblotting with anti-Beclin-1 or anti-MDA-7/IL-24 antibody, respectively, confirmed an interaction between these proteins

(Fig. 6B, upper panel). Double immunofluorescence studies using confocal microscopy further confirmed the interaction of MDA-7/IL-24 and Beclin-1 in DU-145 cells (Fig. 6B, lower panel). The overlapping localization of the two proteins was visible as intense yellow in the merged image. The role of the antiapoptotic proteins, Bcl-2 and Bcl-x_L, on Beclin-1 in switching autophagy to apoptosis in Ad.*mda*-7-infected DU-145 cells was interrogated by immunoprecipitation assays (Supplementary Fig. 4A). The results indicated that Beclin-1 did not interact with either Bcl-2 or Bcl-x_L in the presence of MDA-7/IL-24 thereby nullifying the effect of these proteins in Ad.*mda*-7-induced apoptosis.

To determine the role of ATG5 in the predominantly apoptotic phase at 48 h post-Ad.*mda*-7 infection, atg5 mRNA and protein expressions were analyzed. At 48 h, Ad.*mda*-7 infection resulted in significant induction in atg5 mRNA levels (Fig. 5D). Although the levels of ATG5 protein did not significantly change upon Ad.*mda*-7 infection, a second band corresponding to a molecular weight 24-kDa protein was observed in Ad.*mda*-7-infected groups (Fig. 6A). A recent report indicates that apoptosis is associated with calpain-mediated Atg5 cleavage, resulting in an amino-terminal cleavage product with a relative molecular mass of 24-kDa (43). In this context, calpain activity was measured in Ad.*mda*-7-treated cells by calpain-Glo protease assay. Calpain activity was significantly higher in Ad.*mda*-7-infected cells when compared to control or Ad.*vec*-infected cells (Fig. 6C). We also determined if calpain activation by ER stress induced calcium mobilization following Ad.*mda*-7 infection. Ad.*mda*-7 enhanced calcium release as compared to control Ad.*vec* infected cells and this calcium release was inhibited by calbindin (Supplementary Fig. 4B).

Discussion

mda-7/IL-24 has significant potential as an anti-cancer therapeutic because of its multiplicity of antitumor properties, its non-toxic effects to normal cells and tissues, and its safety and efficacy as observed in a clinical trial (5–8). In the present study, we document that Ad.*mda*-7-induced ER stress and ceramide production lead to early autophagy that subsequently switches to apoptosis in human prostate cancer cells (Fig. 6D). Our experimental evidences indicate that autophagy induced by Ad.*mda*-7 might initially serve a cytoprotective function and inhibition of autophagy by 3-MA augments apoptosis-induction by Ad.*mda*-7. Accordingly, by combining Ad.*mda*-7 with autophagy inhibitors it may be possible to augment the antitumor properties of Ad.*mda*-7 resulting in an improved therapeutic index for patients with prostate cancer. Although potential protective functions of autophagy with respect to Ad.*mda*-7 action have been observed in specific malignant glioma and leukemia cells (21, 44), the mechanism by which this process switches to apoptosis has until now not been mechanistically resolved.

Our experiments demonstrate that Ad.*mda*-7 first induces autophagy selectively in different types of human prostate cancer cells, without promoting this effect in immortal normal human prostate epithelial cells (Fig. 1; Supplementary Fig. 2). We presently demonstrate that autophagy in prostate cancer cells is a consequence of ER stress and ceramide generation, two processes also induced by Ad.*mda*-7 (20,45). The reason Ad.*mda*-7 does not induce these changes in normal cells even in the presence of abundant levels of MDA-7/IL-24 protein remains an enigma. Efforts to decipher this phenomenon will provide further insights into the molecular mechanism of *mda*-7/IL-24 action.

Ceramide is an important second messenger molecule involved in signaling pathways that control cell proliferation, differentiation, death and autophagy (34,35). Ceramide induced by Ad.*mda*-7 controls autophagy by interfering with two pathways encompassing PI3Ks. Class I PI3K and class III PI3K products have been reported to paradoxically inhibit and stimulate autophagy, respectively (Fig. 2C,Fig. 3C). Ceramide reverts the inhibition of the class I PI3K

signaling pathway on autophagy by interfering with IL-13-dependent activation of protein kinase B (PKB) and stimulation of beclin 1 expression (34). Additionally, low doses of radiation induce protective autophagy in breast cancer cells (46). From these results, it is possible that ceramide could be involved in triggering an autophagic response to protect cells during the initial 24 h of Ad.*mda*-7 treatment, whereas a more intense stimulus (48 h after treatment) causes prostate cancer cell death by apoptosis. These findings differ from the effect of high doses of GST-MDA-7 in glioma and renal cells where it induces toxic autophagy (21,22). A possible explanation might be cell type-specificity of action of *mda*-7/IL-24. Alternatively, the disparate response may reflect subtle differences in the mechanism of antitumor action of GST-MDA-7 (versus secreted MDA-7/IL-24 protein) that does not induce autocrine induction of endogenous *mda*-7/IL-24 (18,19) and exerts its anti-cancer activity without dependence on canonical MDA-7/IL-24 receptors (47).

Cellular stress can promote autophagy and apoptosis in multiple ways including induction of autophagy/apoptosis sequentially, simultaneously, or in a mutually exclusive manner (29,48). Interestingly, our data demonstrates that Ad.*mda*-7-induced autophagy and apoptosis occur in a sequential manner and are mutually exclusive with an initial induction of autophagy followed by apoptosis. The switch between autophagy and apoptosis is a complicated process that is currently poorly defined. It was shown that calpain-mediated cleavage of ATG5 is a critical pro-apoptotic event, which activates caspase-dependent cell death (43). Recently, Beclin-1 has been shown to be a substrate for caspases and down-regulation of Beclin-1 expression sensitizes cells to apoptotic cell death (49). In another study, stimulation of the cell death signal by ceramide degrades the autophagy-related proteins Beclin-1 and ATG5 (50), which subsequently induces caspase-dependent apoptosis. We presently demonstrate that 48 h after Ad.*mda*-7 infection protective autophagy shifts to apoptosis that is regulated by Beclin-1 and ATG5. During this predominantly apoptotic phase of Ad.*mda*-7-treatment the interaction between Beclin-1 and MDA-7/IL-24 might inhibit autophagy. At this time, Ad.*mda*-7 increased calpain activity leads to the cleavage of ATG5 and production of a 24-kDa molecular weight product, which might translocate from the cytosol to the mitochondria and be involved in apoptosis (43). Taken together, this study provides new insights into the complex nature of ER stress and ceramide response that may be involved in switching Ad.*mda*-7-induced protective autophagy to apoptosis by regulation of autophagy-related proteins (Fig. 6D).

Our study suggests a novel role for Beclin-1 and ATG5 in mediating a switch between protective autophagy and apoptosis in prostate cancer cells infected with Ad.*mda*-7. These studies implicate calpain activation, which can cleave ATG5 resulting in a 24-kDa truncated protein, as a major contributor to this physiological switch between protective autophagy and apoptosis both of which are promoted by *mda*-7/IL-24 in prostate cancer cells. They also raise a number of intriguing questions. Does the interaction between MDA-7/IL-24 and Beclin-1, or ATG5 cleavage play a role in immune cell development and maturation? Do these interactions or changes in pro-autophagic molecules play any role in inflammatory responses? Further studies aimed at unraveling these newer aspects of MDA-7/IL-24 function would appear valuable. Moreover, based on our present observations, employing strategies to block autophagy through promoting ER stress and ceramide production may represent a viable tactic for enhancing the antitumor activity of *mda*-7/IL-24 toward prostate and potentially other cancers.

Supplementary Material

Refer to Web version on PubMed Central for supplementary material.

Acknowledgments

Supported by NIH NCI grants R01 CA097318 (PBF), R01 CA127641 (PBF), P01 CA104177 (PBF, PD, DTC), and the National Foundation for Cancer Research (NFCR) (PBF). DS is a Harrison Endowed Scholar and PBF holds the Thelma Newmeyer Corman Endowed Chair in Cancer Research in the VCU Massey Cancer Center.

References

1. Jiang H, Lin JJ, Su ZZ, Goldstein NI, Fisher PB. Subtraction hybridization identifies a novel melanoma differentiation associated gene, *mda-7*, modulated during human melanoma differentiation, growth and progression. Oncogene 1995;11:2477–86. [PubMed: 8545104]
2. Sauane M, Gopalkrishnan RV, Sarkar D, et al. MDA-7/IL-24: novel cancer growth suppressing and apoptosis inducing cytokine. Cytokine Growth Factor Rev 2003;14:35–51. [PubMed: 12485618]
3. Pestka S, Krause CD, Sarkar D, Walter MR, Shi Y, Fisher PB. Interleukin-10 and related cytokines and receptors. Annu Rev Immunol 2004;22:929–79. [PubMed: 15032600]
3. Gupta P, Su ZZ, Lebedeva IV, et al. *mda-7*/IL-24: Multifunctional cancer-specific apoptosis-inducing cytokine. Pharmacol Ther 2006;111:596–628. [PubMed: 16464504]
4. Fisher PB, Gopalkrishnan RV, Chada S, et al. *mda7-7*/IL-24, a novel cancer selective apoptosis inducing cytokine gene: from the laboratory into the clinic. Cancer Biol Ther 2003;2:S23–37. [PubMed: 14508078]
5. Fisher PB. Is *mda-7*/IL-24 a “magic bullet” for cancer? Cancer Res 2005;65:10128–38. [PubMed: 16287994]
6. Lebedeva IV, Sauane M, Gopalkrishnan RV, et al. *mda-7*/IL-24: exploiting cancer's Achilles' heel. Mol Ther 2005;11:4–18. [PubMed: 15585401]
7. Cunningham CC, Chada S, Merritt JA, et al. Clinical and local biological effects of an intratumoral injection of *mda-7* (IL24; INGN 241) in patients with advanced carcinoma: a phase I study. Mol Ther 2005;11:149–59. [PubMed: 15585416]
8. Tong AW, Nemunaitis J, Su D, et al. Intratumoral injection of INGN 241, a nonreplicating adenovector expressing the melanoma-differentiation associated gene-7 (*mda-7*/IL24): biologic outcome in advanced cancer patients. Mol Ther 2005;11:160–72. [PubMed: 15585417]
9. Fisher PB, Sarkar D, Lebedeva IV, et al. Melanoma differentiation associated gene-7/interleukin-24 (mda-7/IL-24): Novel gene therapeutic for metastatic melanoma. Toxicol Appl Pharmacol 2007;224:300–7. [PubMed: 17208263]
10. Lebedeva IV, Emdad L, Su ZZ, et al. mda-7/IL-24, novel anticancer cytokine: focus on bystander antitumor, radiosensitization and antiangiogenic properties and overview of the phase I clinical experience. Intl J Oncol 2007;31:985–1007.
11. Sarkar D, Lebedeva IV, Gupta P, et al. Melanoma differentiation associated gene-7 (*mda*-7)/IL-24: a `magic bullet' for cancer therapy? Expert Opin Biol Ther 2007;7:577–586. [PubMed: 17477796]
12. Eager R, Harle L, Nemunaitis J. Ad-MDA-7; INGN 241: a review of preclinical and clinical experience. Expert Opinion Biol Ther 2008;8:1633–43.
13. Ramesh R, Mhashilkar AM, Tanaka F, et al. Melanoma differentiation-associated gene 7/interleukin (IL)-24 is a novel ligand that regulates angiogenesis via the IL-22 receptor. Cancer Res 2003;63:5105–13. [PubMed: 12941841]
14. Miyahara R, Banerjee S, Kawano K, et al. Melanoma differentiation-associated gene-7 (*mda-7*)/ interleukin (IL)-24 induces anticancer immunity in a syngeneic murine model. Cancer Gene Ther 2006;13:753–61. [PubMed: 16543916]
15. Gao P, Sun X, Chen X, et al. Secretable chaperone Grp170 enhances therapeutic activity of a novel tumor suppressor, mda-7/IL-24. Cancer Res 2008;68:3890–8. [PubMed: 18483274]
16. Su ZZ, Lebedeva IV, Sarkar D, et al. Ionizing radiation enhances therapeutic activity of *mda*-7/IL-24: overcoming radiation- and *mda*-7/IL-24-resistance in prostate cancer cells overexpressing the antiapoptotic proteins bcl-x_L or bcl-2. Oncogene 2006;25:2339–48. [PubMed: 16331261]
17. Yacoub A, Hamed H, Emdad L, et al. MDA-7/IL-24 plus radiation enhance survival in animals with intracranial primary human GBM tumors. Cancer Biol Ther 2008;7:917–33. [PubMed: 18376144]

18. Sauane M, Su ZZ, Gupta P, et al. Autocrine regulation of *mda*-7/IL-24 mediates cancer-specific apoptosis. Proc Natl Acad Sci USA 2008;105:9763–8. [PubMed: 18599461]
19. Su ZZ, Emdad L, Sauane M, et al. Unique aspects of *mda-7*/IL-24 antitumor bystander activity: establishing a role for secretion of MDA-7/IL-24 protein by normal cells. Oncogene 2005;24:7552–66. [PubMed: 16044151]
20. Gupta P, Walter MR, Su ZZ, et al. BiP/GRP78 is an intracellular target for MDA-7/IL-24 induction of cancer-specific apoptosis. Cancer Res 2006;66:8182–91. [PubMed: 16912197]
21. Park MA, Yacoub A, Sarkar D, et al. PERK-dependent regulation of MDA-7/IL-24-induced autophagy in primary human glioma cells. Autophagy 2008;4:513–5. [PubMed: 18299661]
22. Yacoub A, Hamed HA, Allegood J, et al. PERK-dependent regulation of ceramide synthase 6 and thioredoxin play a key role in *mda*-7/IL-24-induced killing of primary human glioblastoma multiforme cells. Cancer Res 2010;70:1120–9. [PubMed: 20103619]
23. Park MA, Walker T, Martin AP, et al. MDA-7/IL-24-induced cell killing in malignant renal carcinoma cells occurs by a ceramide/CD95/PERK-dependent mechanism. Mol Cancer Ther. (in press).
24. Eisenberg-Lerner A, Kimchi A. The paradox of autophagy and its implication in cancer etiology and therapy. Apoptosis 2009;14:376–91. [PubMed: 19172397]
25. Scarlatti F, Granata R, Meijer AJ, Codogno P. Does autophagy have a license to kill mammalian cells? Cell Death Differ 2009;16:12–20. [PubMed: 18600232]
26. Gozuacik D, Kimchi A. Autophagy as a cell death and tumor suppressor mechanism. Oncogene 2004;23:2891–6. [PubMed: 15077152]
27. Kanzawa T, Germano IM, Komata T, Ito H, Kondo Y, Kondo S. Role of autophagy in temozolomide-induced cytotoxicity for malignant glioma cells. Cell Death Differ 2004;11:448–57. [PubMed: 14713959]
28. Ellinton AA, Berhow MA, Singletary KW. Inhibition of Akt signaling and enhanced ERK1/2 activity are involved in induction of macroautophagy by triterpenoid B-group soyasaponins in colon cancer cells. Carcinogenesis 2006;27:298–306. [PubMed: 16113053]
29. Carew JS, Nawrocki ST, Kahue CN, et al. Targeting autophagy augments the anticancer activity of the histone deacetylase inhibitor SAHA to overcome Bcr-Abl-mediated drug resistance. Blood 2007;110:313–22. [PubMed: 17363733]
30. Abedin MJ, Wang D, McDonnell MA, Lehmann U, Kelekar A. Autophagy delays apoptotic death in breast cancer cells following DNA damage. Cell Death Differ 2007;14:500–10. [PubMed: 16990848]
31. Levine B, Kroemer G. Autophagy in pathogenesis of disease. Cell 2008;132:27–42. [PubMed: 18191218]
32. Ogata M, Hino S, Saito A, et al. Autophagy is activated for cell survival after endoplasmic reticulum stress. Mol Cell Biol 2006;26:9220–31. [PubMed: 17030611]
33. Ding WX, Ni HM, Gao W, et al. Differential effects of endoplasmic reticulum stress-induced autophagy on cell survival. J Biol Chem 2007;282:4702–10. [PubMed: 17135238]
34. Scarlatti F, Bauvy C, Ventruti A, et al. Ceramide-mediated macroautophagy involves inhibition of protein kinase B and up-regulation of beclin 1. J Biol Chem 2004;279:18384–91. [PubMed: 14970205]
35. Bursch W, Hochegger K, Torok L, et al. Autophagic and apoptotic types of programmed cell death exhibit different fates of cytoskeletal filaments. J Cell Sci 2000;113:1189–98. [PubMed: 10704370]
36. Bae VL, Jackson-Cook CK, Brothman AR, Maygarden SJ, Ware JL. Tumorigenicity of SV40 T antigen immortalized human prostate epithelial cells: association with decreased epidermal growth factor receptor (EGFR) expression. Int J Cancer 1994;58:721–29. [PubMed: 8077059]
37. Lebedeva IV, Sarkar D, Su ZZ, et al. Bcl-2 and Bcl-x(L) differentially protect human prostate cancer cells from induction of apoptosis by melanoma differentiation associated gene-7, mda-7/IL-24. Oncogene 2003;22:8758–73. [PubMed: 14647471]
38. Cheng Y, Qiu F, Ye YC, et al. Autophagy inhibits reactive oxygen species-mediated apoptosis via activating p38-nuclear factor-kappa B survival pathways in oridonin-treated murine fibrosarcoma L929 cells. FEBS J 2009;276:1291–1306. [PubMed: 19187231]
39. Tormo D, Checińska A, Alonso-Curbelo D, et al. Targeted activation of innate immunity for therapeutic induction of autophagy and apoptosis in melanoma cells. Cancer Cell 2009;16:103–14. [PubMed: 19647221]

40. Criollo A, Maiuri MC, Tasdemir E, et al. Regulation of autophagy by the inositol trisphosphate receptor. Cell Death Differ 2007;14:1029–39. [PubMed: 17256008]
41. Sarkar D, Lebedeva IV, Su ZZ, et al. Eradication of therapy-resistant human prostate tumors using a cancer terminator virus. Cancer Res 2007;67:5434–42. [PubMed: 17545625]
42. Shimizu S, Kanaseki T, Mizushima N, et al. Role of Bcl-2 family proteins in a non-apoptotic programmed cell death dependent on autophagy genes. Nat Cell Biol 2004;6:1221–8. [PubMed: 15558033]
43. Yousefi S, Perozzo R, Schmid I, et al. Calpain-mediated cleavage of Atg5 switches autophagy to apoptosis. Nat Cell Biol 2006;8:1124–32. [PubMed: 16998475]
44. Yang C, Tong Y, Ni W, et al. Inhibition of autophagy induced by overexpression of *mda*-7/IL-24 strongly augments the antileukemic activity *in vitro* and *in vivo*. Cancer Gene Ther. 2009 in press.
45. Sauane M, Su Z-z, Dash R, et al. Ceramide plays a prominent role in MDA-7/IL-24-induced cancer-specific apoptosis. J Cell Physiol. 2009 in press.
46. Paglin S, Hollister T, Delohery T, et al. A novel response of cancer cells to radiation involves autophagy and formation of acidic vesicles. Cancer Res 2001;61:439–44. [PubMed: 11212227]
47. Sauane M, Gopalkrishnan R, Choo HT, et al. Mechanistic aspects of *mda*-7/IL-24 cancer cell selectivity analyzed via a bacterial fusion protein. Oncogene 2004;23:7679–90. [PubMed: 15334067]
48. Xue L, Fletcher GC, Tolkovsky AM. Mitochondria are selectively eliminated from eukaryotic cells after blockade of caspases during apoptosis. Curr Biol 2001;11:361–65. [PubMed: 11267874]
49. Cho DH, Jo YK, Hwang JJ, et al. Caspase-mediated cleavage of ATG6/Beclin-1 links apoptosis to autophagy in HeLa cells. Cancer Lett 2009;274:95–100. [PubMed: 18842334]
50. Fujiwara K, Daido S, Yamamoto A, et al. Pivotal role of the cyclin-dependent kinase inhibitor p21WAF1/CIP1 in apoptosis and autophagy. J Biol Chem 2008;283:388–97. [PubMed: 17959603]

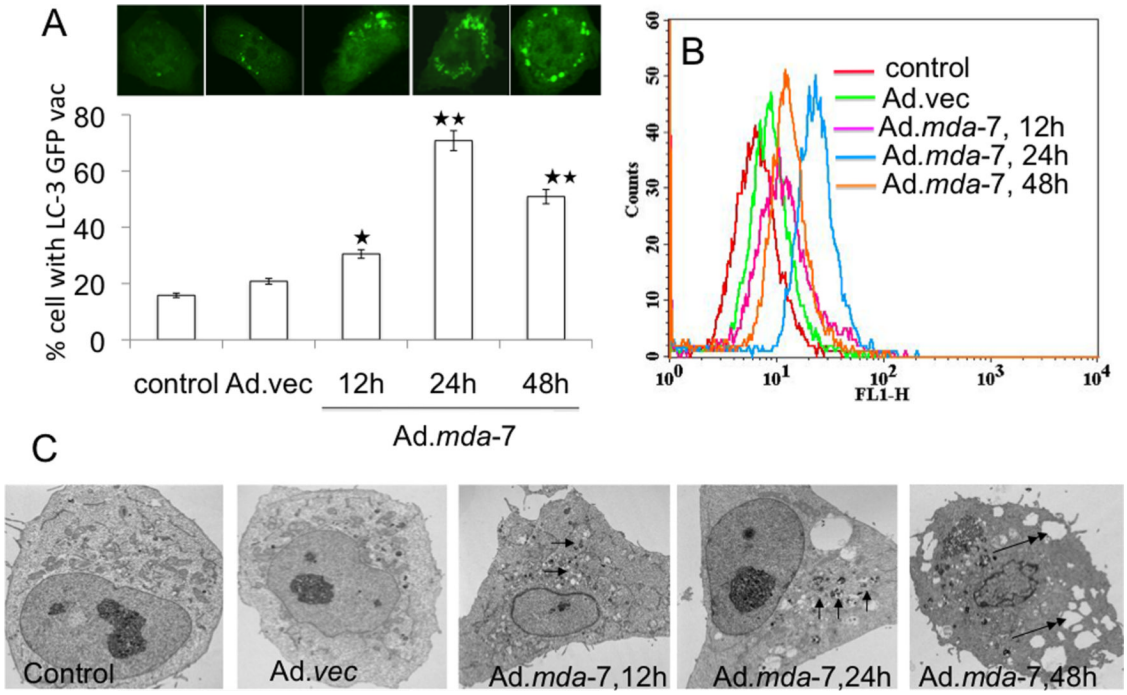

Fig. 1. MDA-7/IL-24 induces autophagy in DU-145 cells

A, DU-145 cells were transfected with GFP-LC3 and infected with Ad.*mda*-7 (100pfu/cell) and after different times localization of LC3 in transfected cells was examined by confocal microscopy (magnification ×100) and autophagosome formation was quantified and data presented as percentage of GFP-LC3–transfected cells with punctate fluorescence to autophagosome formation. A minimum of 100 GFP-LC3–transfected cells were counted. *, $P < 0.05$; **, $P < 0.001$, compared with control at the corresponding time. B, The MDC fluorescent intensity of Ad.*mda*-7-treated DU-145 cells was analyzed by flow cytometry. This result was representative of three different experiments. C, DU-145 cells were infected with 100 pfu/cell of Ad.*mda*-7 or Ad.*vec* for different times and cells were fixed and processed for electron microscopy (single arrow, autophagosome; double arrow, empty vacuole; Scale bars: control and others-2μm).

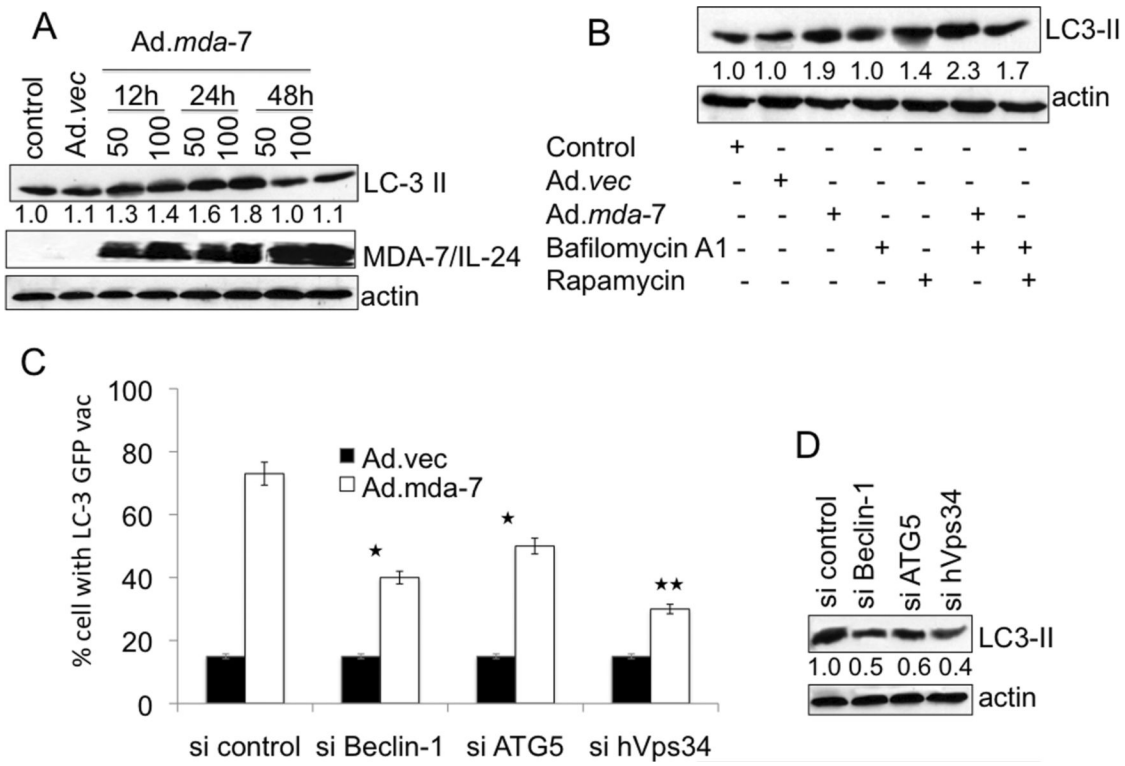

Fig. 2. MDA-7/IL-24 induces canonical autophagy in DU-145 cells

A, DU-145 cells were infected with Ad.*mda*-7 or Ad.*vec* for different times and LC3 expression was analyzed by Western blotting. B, LC3 expression was examined after 24 h treatment with Ad.*mda*-7 or Ad.*vec* (100 pfu/cell) in the presence of rapamycin (100 nM), or bafilomycin A1 (100 nM). C, Cells were transfected with the indicated siRNAs and LC3-GFP followed by infection with 100 pfu/cell Ad.*mda*-7 or Ad.*vec* and cytoplasmic aggregation of LC3-GFP was determined. A minimum of 100 GFP-LC3–transfected cells were counted. *, $P < 0.05$; **, $P < 0.001$, compared with si control. D, LC3-II expression 24 h after administration of the indicated siRNAs and Ad.*mda*-7 infection (100 pfu/cell) by immunoblot. Densitometry was performed on the original blots, and the ratio of LC3-II/actin in control cells was 1.

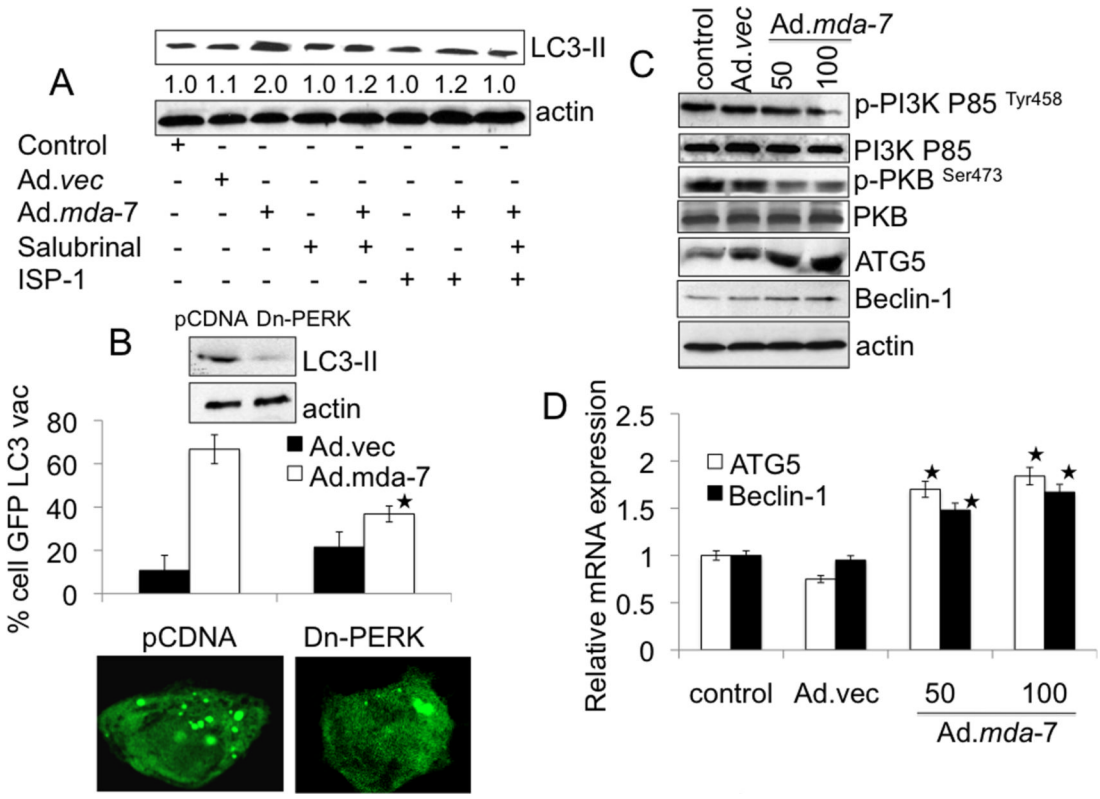

Fig. 3. MDA-7/IL-24-induced autophagy is mediated through ER stress and ceramide production

A, DU-145 cells were infected with 100 pfu/cell of Ad.*mda*-7 or Ad.*vec* in the presence of Salubrinal (5 μM) and/or ISP-1 (10 μM) for 24 h followed by analysis of LC3 expression by immunoblotting. Densitometry was performed on the original blots, and the ratio of LC3-II/actin in control cells was 1. B, DU-145 cells were transfected with the indicated plasmids: empty vector control plasmid (pCDNA) or a plasmid expressing dominant negative PERK (Dn-PERK) and GFP-LC3. Cells were analyzed for LC3 aggregation and LC3 expression 24 h after Ad.*mda*-7 or Ad.*vec* infection (100 pfu/cell). *, $P < 0.05$; compared with pCDNA Ad.*mda*-7 infected cells. C, Evaluation of protein expression: Beclin-1, ATG5, total PKB, p-PKB, total PI3K and p-PI3K using immunoblotting 24 h after Ad.*mda*-7 or Ad.*vec* infection (100 pfu/cell). D, DU-145 cells were infected with 100 pfu/cell of Ad.*mda*-7 or Ad.*vec* and after 24 h expression of Beclin-1 and ATG5 mRNA was determined using Taqman real-time PCR. Values are the mean ± S.D. of three independent experiments and *, $p < 0.05$ versus control cells.

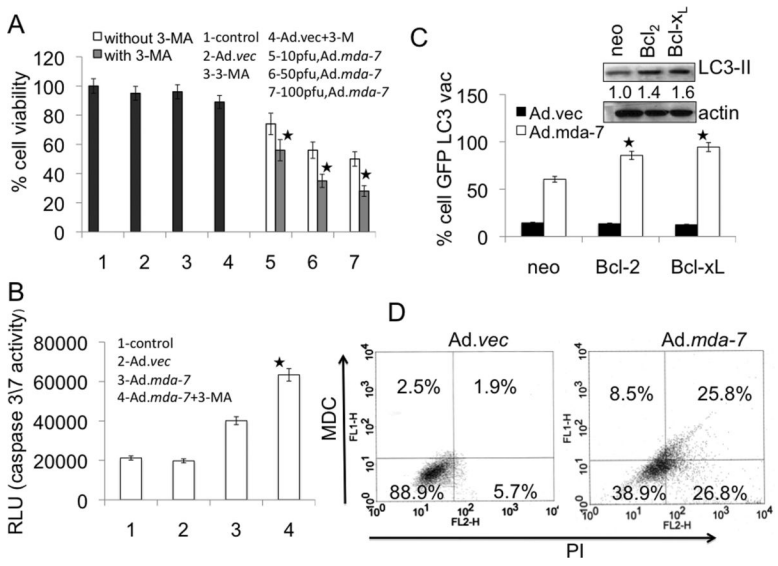

Fig. 4. Relationship between autophagy and apoptosis induced by Ad.*mda*-7

A, MTT assay after infection with Ad.*mda*-7 or Ad.*vec* (different pfu/cell) for 48 h in absence or presence of 3-MA (10 mM for 48 h). B, Caspase-Glo(R) 3/7 assay analyses for caspase-3 expression in DU-145 cells infected with Ad.*mda*-7 or Ad.*vec* (100 pfu/cell) for 48 h in absence or presence of 3-MA (10 mM, 48 h). Values are the mean ± S.D. of three independent experiments. *, $p < 0.05$ versus only Ad.*mda*-7-treated cells. C, Bcl-2 and Bcl-x_L overexpressed DU-145 cells were infected with Ad.*mda*-7 or Ad.*vec* (100 pfu/cell) for 24 h and analyzed for LC3 aggregation and LC3 expression by immunoblotting. *, $p < 0.05$ versus Ad.*mda*-7-treated DU-Neo cells. Densitometry was performed on the original blots, and the ratio of LC3-II/actin in Ad.*mda*-7-treated neo cells was 1. D, DU-145 cells were infected with Ad.*mda*-7 or Ad.*vec* (100 pfu/cell) for 48 h and stained with MDC and PI followed by flow cytometric analysis. This result was representative of three different experiments.

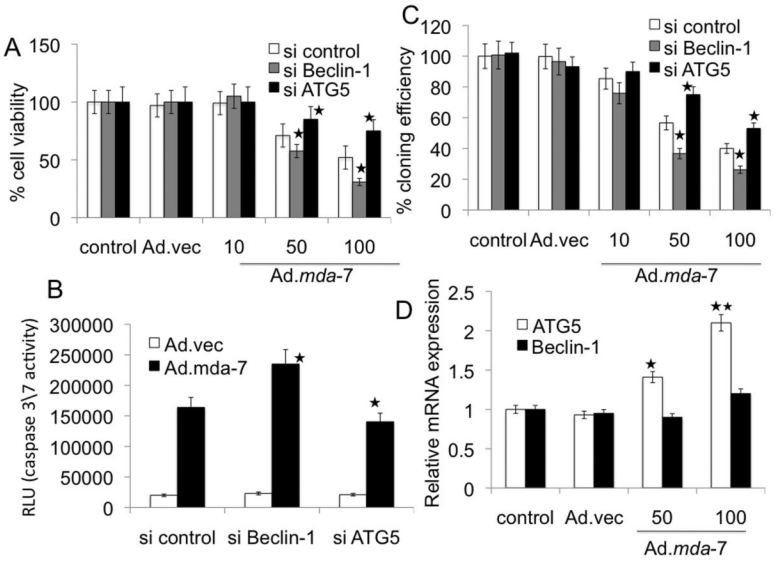

Fig. 5. Role of Beclin-1 and ATG5 in Ad.*mda*-7-induced apoptosis

DU-145 cells were transfected with the indicated siRNAs and cell viability was determined by MTT assay (A), Caspase-Glo(R) 3/7 assay (B) for caspase-3 expression and colony formation assays (C) 48 h after infection with Ad.*mda*-7 (10, 50 or 100 pfu/cell) or Ad.*vec* (100 pfu/cell). C, Colony formation assays in monolayer culture. Colonies were fixed, stained and counted (> 50 cells) 2 weeks after plating. D, Expression profile of Beclin-1 and ATG5 at the mRNA level 48 h after Ad.*mda*-7-infection (50 or 100 pfu/cell) of DU-145 cells (*, $P < 0.05$; **, $P < 0.001$, compared with control).

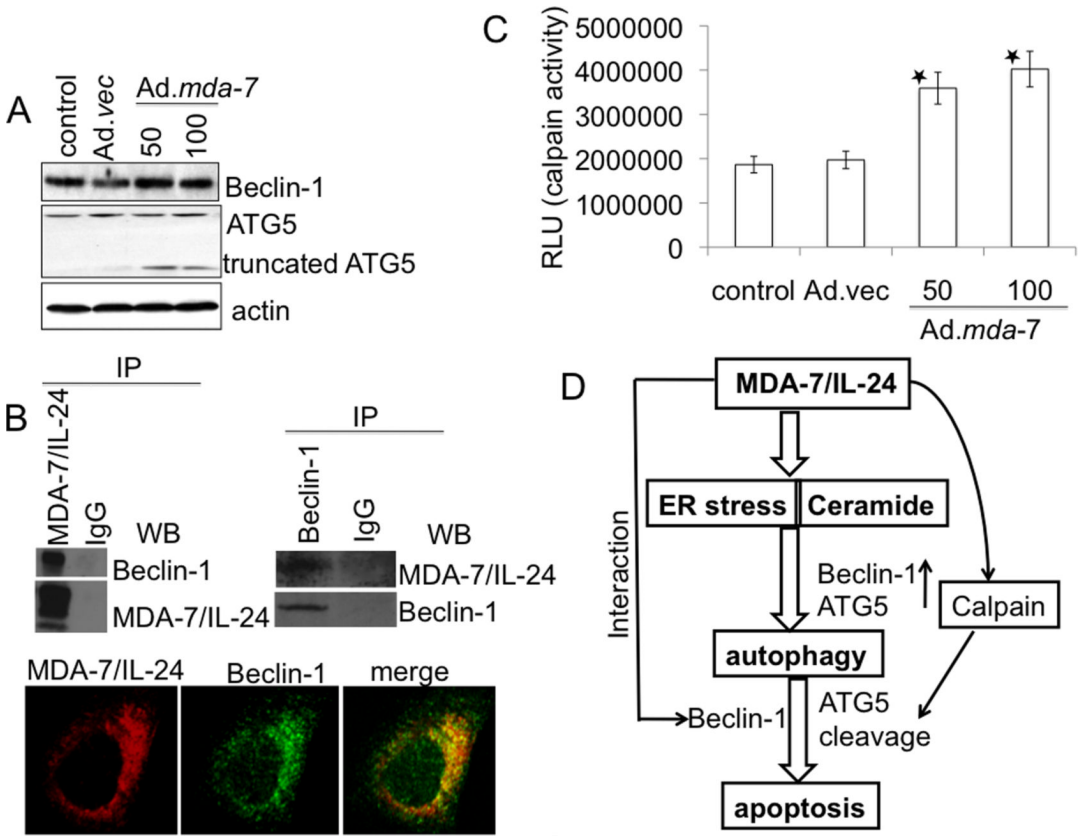

Fig. 6. Role of Beclin-1 and ATG-5 in Ad.*mda*-7-induced apoptosis

A, Expression profile of Beclin-1 and ATG5 protein levels 48 h post-infection of DU-145 cells with Ad.*mda*-7 (50 or 100 pfu/cell) or Ad.*vec* (100 pfu/cell). B, DU-145 cells were infected with 100 pfu/cell of Ad.*vec* or Ad.*mda*-7 for 48 h and immunoprecipitated with anti-MDA-7/IL-24 or anti-Beclin-1 followed by immunoblotting with anti-Beclin-1 or anti-MDA-7/IL-24 antibodies (upper panel). Fluorescent confocal micrographs of DU-145 showing co-immunolocalization of Beclin-1 and MDA-7/IL-24 (lower panel). C, DU-145 cells were infected with Ad.*vec* (100 pfu/cell) or Ad.*mda*-7 (50 or 100 pfu/cell) for 48 h followed by calpain assay using calpain-Glo assay. Values reported are mean ± S.D. of three independent experiments. *, $p < 0.05$ versus control cells. D, Model illustrating the possible molecular mechanism of ER stress- and ceramide-mediated autophagy promoted by MDA-7/IL-24 that switches to apoptosis in prostate cancer cells.